DESIGN AND FABRICATION OF AN AUTOMATED COMPLETE DEFLASHING MACHINE FOR HDPE PLASTIC BOTTLES

THIẾT KẾ VÀ CHẾ TẠO MÁY XỬ LÝ TOÀN BỘ BAVIA TỰ ĐỘNG CHO CHAI NHỰA HDPE

Tan Minh Nguyen, Xuan Nguyen Nguyen, Quang Hieu Tran, Viet Doan Le, Quoc Loi Tran, Van Dat Pham, Tran Anh Vo*, Minh Sang Tran

The University of Danang - University of Science and Technology, Vietnam

*Corresponding author: vtanh@dut.udn.vn

(Received: February 09, 2026; Revised: March 16, 2026; Accepted: March 19, 2026)

DOI: 10.31130/ud-jst.2026.24(5A).089

Abstract - During HDPE bottle production via extrusion blow molding (EBM), flash typically forms at the bottle bottom, neck, and mold parting lines. Removing this flash is essential for dimensional accuracy, surface quality, and product functionality. However, in many production lines, this operation remains manual or semi-automated, resulting in low throughput and inconsistent quality. This study presents the design and fabrication of an automated deflashing machine for HDPE bottles that integrates clamping, positioning, and rotary cutting mechanisms to remove flash at both the bottle bottom and neck within a single compact system. The machine employs rack-and-pinion-driven assemblies with pneumatic actuation, allowing flexible adaptation to various bottle sizes and wall thicknesses. Experimental results demonstrate stable operation at approximately 700 bottles per hour for bottles with a diameter of 60 mm, height of 70 mm, and wall thickness of 0.4 mm, confirming the system's strong viability for practical deployment in industrial EBM production lines.

Key words - Extrusion blow molding; Deflashing machine; HDPE bottle; Cutting mechanism; Automation.

Tóm tắt – Trong quá trình sản xuất chai HDPE bằng công nghệ thổi đùn (EBM), bavia thường hình thành tại đáy, cổ chai và đường phân khuôn. Loại bỏ bavia là bắt buộc để đảm bảo độ chính xác kích thước, chất lượng bề mặt và chức năng sản phẩm. Tuy nhiên, nguyên công này tại nhiều dây chuyền vẫn thực hiện thủ công hoặc bán tự động, gây năng suất thấp và chất lượng không đồng đều. Nghiên cứu này giới thiệu thiết kế, chế tạo máy cắt bavia tự động cho chai HDPE, tích hợp cơ cấu kẹp chặt, định vị và cắt xoay để làm sạch bavia đáy và cổ chai trong một hệ thống nhỏ gọn. Thiết bị ứng dụng cơ cấu truyền động bánh răng - thanh răng kết hợp dẫn động khí nén, giúp thích ứng linh hoạt với nhiều kích cỡ và độ dày thành chai. Kết quả thực nghiệm chứng minh máy vận hành ổn định đạt năng suất khoảng 700 chai/giờ đối với chai đường kính 60 mm, cao 70 mm, dày thành 0.4 mm; khẳng định tính khả thi cao khi triển khai thực tế trên các dây chuyền EBM công nghiệp.

Từ khóa – Thổi đùn; Máy cắt bavia; Chai HDPE; Cơ cấu cắt; Tự động hóa.

1. Introduction

Plastic materials, particularly high-density polyethylene (HDPE), continue to be widely used in industrial manufacturing and daily applications owing to their favorable properties. The rising demand for polyethylene in the chemical, automotive, and consumer packaging industries has driven a corresponding increase in products manufactured by extrusion blow molding (EBM) technology. After injection molding and extrusion, blow molding is one of the most widely used manufacturing methods for producing polymer parts [1]. Polymer parts, especially plastic bottles, manufactured by the EBM method exhibit characteristic flash at the bottle neck and bottom, with varying morphologies depending on the mold pinch-off configuration used at the production site. Flash generation is an inherent feature of this process.

Previous studies and solutions have mainly focused on removing flash at a single location on the product, such as the bottle neck or the bottom region of extrusion-blown plastic bottles. Many deflashing devices have been specifically designed to remove flash at the neck of the bottle through rotary mechanisms or specialized cutting blades [2], [3], [4], [5]. Some other systems employ rotary deflashing mechanisms or rotating blades to improve production throughput; however, these devices still remove flash at individual locations on the product [6], [7], [8]. Therefore, when flash must be removed at multiple locations, the production process often requires multiple stages or different deflashing devices.

In addition, many existing deflashing devices have been developed as standalone mechanical modules, in which the functions of clamping, positioning, and flash removal are often performed by separate mechanisms or through multiple processing steps [9], [10], [11]. Some systems apply continuous-motion mechanisms to improve productivity; however, they often require complex multi-mechanism coordination within a single system [12]. These characteristics may increase the complexity of the equipment and make integration into production lines more difficult.

Furthermore, some solutions have been proposed to handle special bottle configurations, such as twin bottles or connected containers formed during the molding process [13], [14]. Although these designs may satisfy specific technical requirements, they often lead to complex mechanical structures and high fabrication costs, thereby limiting their widespread adoption in industrial manufacturing.

Recent studies have demonstrated the growing demand for integrating automated mechanical systems into local manufacturing to enhance productivity and product quality [15], [16]. Building upon these findings and addressing the aforementioned limitations, this study proposes the design and fabrication of an integrated, automated deflashing machine that performs sequential flash removal at both the bottle neck and bottom within a single compact system. The mechanical structure is designed for simplicity, ease of manufacture, and flexible adjustment to accommodate various HDPE bottle sizes in production lines.

2. Overview of the extrusion blow molding process

The extrusion blow molding process typically consists of the following main stages: extrusion, mold closing, parison inflation, cooling, and mold opening with part ejection. During the extrusion stage, the molten material is extruded through the die head to form a hollow tube called a parison. Subsequently, the two mold halves close to clamp the parison, and compressed air is introduced into it, causing the parison to inflate and conform to the mold cavity to form the final part geometry. Processing parameters such as melt temperature, blow pressure, extrusion speed, and mold design directly affect the dimensional accuracy and mechanical properties of the product [17], [18].

During mold closing and forming, a portion of the molten material may be forced out at the mold parting line due to blowing pressure and mold clamping force. After cooling, this excess material forms flash at locations such as the bottle body, neck, or bottom. Figure 1 illustrates an HDPE plastic bottle after the extrusion blow molding process, in which flash remains at two characteristic locations, namely the bottle neck and bottle bottom, as a result of the mold pinch-off geometry. Flash formation is a common feature in polymer forming processes and is influenced by many factors such as melt viscosity, parison temperature, blow pressure, and mold dimensional tolerance [1], [17], [19]. In addition, the non-uniform parison wall thickness distribution during inflation may also increase the likelihood of flash formation in regions of the product subjected to large deformation [18]. In the production of HDPE bottles, flash thickness usually depends on processing conditions and mold design.

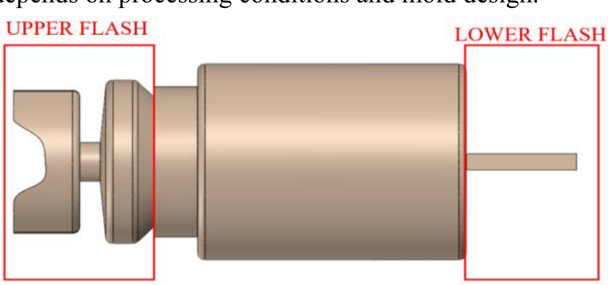

Figure 1. *HDPE bottle after blow molding showing flash at the neck and bottom.*

In addition to the formation mechanism, the mechanical properties of flash also play an important role in post-forming processes, particularly in the deflashing operation. Since flash typically has a small thickness and cools rapidly upon contact with the metal mold surface, its crystalline morphology may differ from that of the part wall. The mechanical properties of polymer materials, such as tensile strength, Young's modulus, and elongation at break, directly affect the force required to remove flash during the deflashing process [18]. In many cases, flash has lower mechanical strength than the part wall, but a minimum cutting force is still required to ensure clean flash separation without deforming the part.

3. Design of the deflashing machine

3.1. Operating principle

Figure 2 shows the movement of the plastic bottle within the machine. The system performs two separate deflashing operations at the bottle bottom and bottle neck. Flash removal at the bottle bottom is carried out by generating relative rotational motion between the bottle body and the flash at the bottle bottom through a rotary assembly driven by a rack-and-pinion mechanism. The bottle is then transferred to the neck-cutting station to remove the flash at the neck by generating relative rotational motion between the bottle and the blade through a rack-and-pinion mechanism. Table 1 presents the bottle specifications that the machine can accommodate for various bottle sizes, with a bottle body diameter of approximately 60–100 mm, a bottle body height excluding the two flash regions of approximately 50–110 mm, and a bottle wall thickness ranging from 0.4 to 0.8 mm.

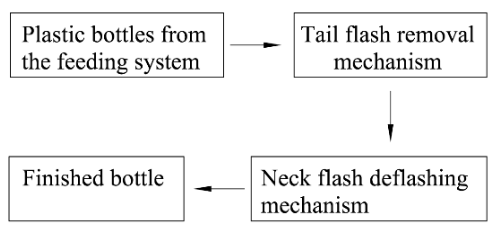

Figure 2. *Diagram of bottle movement within the device*

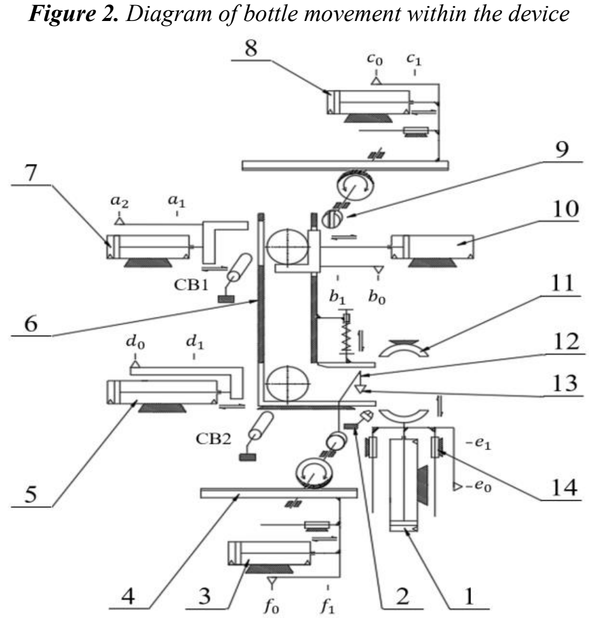

Figure 3. *Principle diagram of the machine*

Figure 3 presents the operating principle of the system. After the extrusion blow molding process, the plastic bottle is introduced into the machine through the guide chute (6), which orients and guides the bottle sequentially to the processing positions. When the bottle reaches the first processing position, sensor (1) detects its presence and activates the clamping unit consisting of pneumatic cylinders (7) and (10) to secure the bottle. The distance between the jaws of this unit can be adjusted to accommodate bottles with different diameters, while the clamping force of the pneumatic cylinders can be adjusted through the regulated air pressure to suit bottles with different wall thicknesses, thereby ensuring that the bottle is securely held without deformation during processing. After the bottle is positioned, cylinder (8) extends linearly and drives the rack-and-pinion mechanism, causing the bottom-deflashing assembly (9) to rotate and separate the flash at the bottle bottom. The installation position of this cutting assembly is designed to be vertically adjustable, allowing the system to process bottles with different heights within the design range.

Table 1. *Bottle specifications that the machine can accommodate*

Specifications	**Value**
Bottle diameter	60 – 100 mm
Bottle height	50 – 110 mm
Bottle wall thickness	0.4 – 0.8 mm

After the bottom-deflashing operation is completed, the bottle continues to move along the guide chute (6) to the second processing position. At this position, sensor (2) detects the bottle and activates cylinder (5) to push the bottle into the clamping unit (11). Next, cylinder (1) extends to clamp and center the bottle before neck deflashing. Similar to the first stage, the distance between the jaws can be adjusted to match the bottle diameter, while the clamping force is adjusted through the pneumatic system to accommodate different bottle wall thicknesses. Then, cylinder (3) extends and drives the rack-and-pinion mechanism (4), causing the blade holder (12) and cutting blade (13) to rotate around the bottle neck to cut off the flash. The height of the cutting assembly is also designed to be adjustable to ensure precise cutting positions for bottles of different heights. After both deflashing operations at the bottle bottom and neck are completed, the finished part is ejected from the working area via the blow-off valve (2) to the next stage in the production line.

3.2. Finite element analysis of the deflashing process

The input parameters were determined from the process requirements of extrusion blow molding and the geometric characteristics of the plastic bottle, including bottle dimensions, wall thickness as presented in Table 1, flash formation locations, and the target throughput of the system. These parameters serve as the basis for constructing the design model and determining the operating conditions of the machine mechanisms.

From these input parameters, the design parameters of the system were determined through mechanical calculations, including cutting force, drive force, rack-and-pinion dimensions, as well as the mass and acceleration of the moving parts.

In the finite element model, the bottle body and flash were modeled as deformable bodies, while the cutting mechanism components were assumed to be rigid bodies in order to reduce computational cost, given the negligible tool deformations. The material model of the bottle was established based on the mechanical properties of HDPE, with the parameters presented in Table 2. The mechanical behavior of the material was described by an elasto-plastic constitutive model, enabling the simulation of deformation and fracture in the flash region during cutting.

Table 2. *Basic properties of HDPE.*

Properties	**Value**
Density	952 kg/m^3
Yield strength	33 MPa
Young’s modulus	1250 MPa

The boundary conditions were established to reproduce the operating principle of the system. For the bottle-bottom deflashing process, the cutting assembly was assigned a prescribed rotational motion about the y-axis, while the bottle body was fully constrained (six degrees of freedom) to ensure model stability. For the bottle-neck deflashing process, the simulation was conducted in two stages. Initially, the blade was assigned a prescribed translational motion to achieve the required depth of cut, while the bottle was fixed. Subsequently, the blade was fully constrained and the bottle was assigned a rotational motion to perform cutting around the bottle neck. This approach creates relative motion equivalent to the case in which the blade rotates, while reducing computational cost and improving numerical stability.

Due to the complex geometry of the bottle body and flash, tetrahedral elements were used to discretize the model. The mesh was refined in the contact region between the flash and the bottle body with an element size of 0.5 mm, while the element size gradually increased away from the contact zone to balance accuracy and computational efficiency. The meshing strategy and simulation model are illustrated in Figures 5 and 7.

To evaluate the effect of variations in the input parameters, particularly bottle wall thickness, a sensitivity analysis was conducted in the range of 0.4–0.8 mm, corresponding to the common wall thickness range of HDPE bottles in practical production. In this study, thickness values of 0.4, 0.5, 0.6, 0.7, and 0.8 mm were selected, while the other model parameters were kept constant.

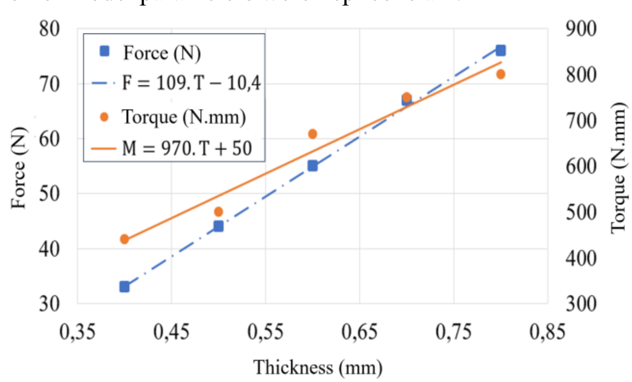

Figure 4. *Linear relationship between cutting force, cutting torque and bottle wall thickness*

Figure 4 shows that when the bottle wall thickness increases from 0.4 mm to 0.8 mm, the cutting force increases from 33 N to 76 N, while the torque increases from 440 N·mm to 800 N·mm. This trend indicates that the cutting force and torque have a linear relationship with material thickness, consistent with the shear failure mechanism, as the shear cross-sectional area increases proportionally. Based on these data, the quantitative relationship between bottle wall thickness and the processing force and torque was established through a linear regression model.

The regression equations obtained for the cutting force and torque are as follows:

$$F = 109.T - 10,4 \quad (1)$$

$$M = 970.T + 50 \quad (2)$$

where F is the cutting force (N), M is the cutting torque (N·mm) and T is the bottle wall thickness (mm).

To evaluate the goodness of fit of the regression model, the coefficient of determination R^2 was used and was determined according to the following equation:

$$R^2 = 1 - \frac{\sum_{i=1}^{n}(y_i - \hat{y}_i)^2}{\sum_{i=1}^{n}(y_i - \bar{y}_i)^2} \quad (3)$$

$y_i, \hat{y}_i, \bar{y}_i$ where is the observed value, is the value predicted by the regression model, and is the mean value of the dataset. The calculated results show that the coefficient of determination of the force model reaches R2=0.998, while that of the torque model reaches R2=0.961. These values are both greater than 0.9, demonstrating that the regression model accurately describes the relationship between bottle wall thickness and the cutting force and torque. This indicates that the simulation model has good stability and predictive capability within the investigated range.

3.3. Calculation of cylinder requirements

3.3.1. Cylinder of the bottle-bottom deflashing mechanism

Contact length between the flash and the bottle body: L= 40 mm

Compressed air pressure: P = 3 bar

Cylinder efficiency: η_C = 0.85

Mass of moving parts: m= 2.5 kg

Acceleration of moving parts: a = 0.2 m/s^2

Pitch radius of the gear: r_G = 15.625 mm

Gear mass: $m_G = 0.1\ kg$

Rotating shaft radius: r_S = 9 mm

Rotating shaft mass: $m_S = 0.7\ kg$

Mass moment of inertia:

$$J = J_{gear} + J_{shaft} = \frac{1}{2}.m_G.r_G^2 + \frac{1}{2}.m_S.r_S^2$$

$$= 4.056.\ 10^{-5}\ (kg.m^2)$$

Rolling friction coefficient: μ = 0.001

Rack-and-pinion efficiency: η_1 = 0.97

η_2Bearing efficiency: = 0.99

F_{ms}=$\mu.m.g$ = 0.025 (N)Rolling friction force on the linear ball-bearing guide assembly of the moving parts:

Required thrust force for the moving-part assembly:

$$F_N = \frac{\left(m + \frac{J}{r_G^2}\right)a + F_{ms}}{\eta_1.\eta_2} = 0.55\ \text{N}$$

The CAE simulation result in Figure 6 shows that the required applied force derived from torque M is:

$$F_C = \frac{M}{L/2} = 300\ \text{N}$$

Required thrust force for the entire bottle-bottom deflashing mechanism:

$$F = F_N + F_C = 300.55\ \text{N}$$

Piston area: $A = \frac{F}{P.\eta_C} = 1.2.10^{-3}\ m^2$

Piston diameter: $D = \sqrt{\frac{4A}{\pi}} = 39.1$ mm (4)

Cylinder stroke: $S = 2.\ r_G.\ \pi$ = 98.17 mm (5)

Based on the calculation results in Eqs. (4) and (5), a pneumatic cylinder of bore Ø40 × stroke 100 mm was selected.

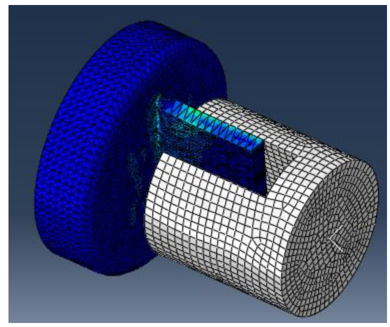

Figure 5. *Mesh distribution and simulation of the bottle-bottom deflashing process*

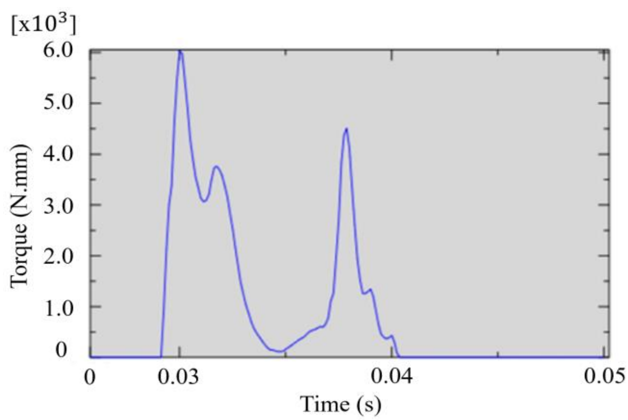

Figure 6. *Torque diagram of the bottle-bottom deflashing process*

3.3.2. Cylinder of the bottle-neck deflashing mechanism

Rotating shaft mass: m_S = 0.2 kg

Bottle neck radius: r = 20 mm

The other parameters are identical to those of the bottle-bottom deflashing mechanism cylinder, as they share similar structures.

Mass moment of inertia:

$$J = J_{gear} + J_{shaft} = \frac{1}{2}.m_G.r_G^2 + \frac{1}{2}.m_S.r_S^2$$

$$= 2.031.10^{-5}\ (kg.m^2)$$

Required thrust force for the moving-part assembly:

$$F_N = \frac{\left(m + \frac{J}{r_G^2}\right)a + F_{ms}}{\eta_1.\eta_2} = 0.55\ \text{N}$$

The CAE simulation result in Figure 4 shows that the required cutting force derived from torque M at a thickness of 0.8 mm is equivalent to the theoretical calculation value.

$F_C = \frac{M}{r} = 40$ N

Required thrust force for the entire bottle-neck deflashing mechanism:

$F = F_N + F_C = 40.55$ N

Piston area: $A = \frac{F}{P.\eta_C} = 1.59.10^{-4}\ m^2$

Piston diameter: $D = \sqrt{\frac{4A}{\pi}} = 14.2$ mm (6)

Cylinder stroke: $S = 2.\ r_G.\ \pi = 98.17$ mm (7)

Based on the calculation results in Eqs. (6) and (7), a pneumatic cylinder of bore Ø20 × stroke 100 mm was selected.

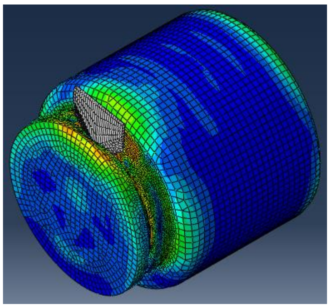

Figure 7. *Mesh distribution and simulation of the bottle-neck deflashing process*

3.3.3. Cylinder of the bottle clamping mechanism

The bottle clamping component is designed to perform the clamping task while simultaneously penetrating into the bottle wall to achieve the required depth of cut for the blade; therefore, the cylinder is calculated based on this penetration force.

Penetration force at a bottle thickness of 0.8 mm:

$F_C = 76$ N

Mass of the clamping fixture: $m = 0.5$ kg

Stroke of the clamping fixture: $S_k = 110$ mm (ensuring accommodation for the largest bottle diameter of 100 mm)

Required clamping force: $F = F_C + m.g = 80.9$ N

Piston area: $A = \frac{F}{P.\eta_C} = 3.17.10^{-4}\ m^2$

Piston diameter: $D = \sqrt{\frac{4A}{\pi}} = 20$ mm (8)

Cylinder stroke: $S = S_k = 110$ mm (9)

Based on the calculation results in Eqs. (8) and (9), a pneumatic cylinder of bore Ø25 × stroke 125 mm was selected.

4. Mechanical design of the deflashing device

4.1. Mechanical design

The deflashing assemblies were designed with similar structures in order to reduce fabrication cost and facilitate assembly. Figures 8 and 9 present the bottle-bottom deflashing assembly and the bottle-neck deflashing assembly, respectively. These assemblies were designed to accommodate various bottle sizes as listed in Table 1. Figure 10 shows the actual machine after completion, with overall dimensions of 600 × 600 × 1000 mm.

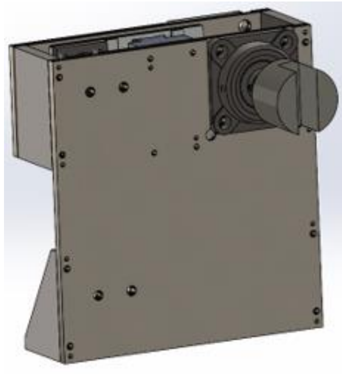

Figure 8. Model of the bottle-*bottom deflashing assembly*

Figure 9. *Model of the bottle-neck deflashing assembly*

Figure 10. *Photograph of the actual machine*

4.2. Machine control system

To control the machine with multiple actuators, the Mitsubishi FX3U PLC was selected as the most suitable option. Owing to its programming flexibility and reasonable cost, this PLC model is widely adopted in industrial automation. Figures 11 and 12 present the GRAFCET sequential function charts of the bottle-bottom and bottle-neck deflashing mechanisms, respectively. These two mechanism assemblies are controlled independently to optimize the deflashing time, enabling continuous operation without creating excessive idle time between bottles. A 24 VDC power supply is used for the PLC and the OP320 A-S HMI control panel. Figure 13 shows the HMI screen interface and the operating buttons.

Electro-pneumatic solenoid valves are used to control the cylinders via the PLC outputs without intermediate relays, as the PLC incorporates built-in relay outputs at its output terminals.

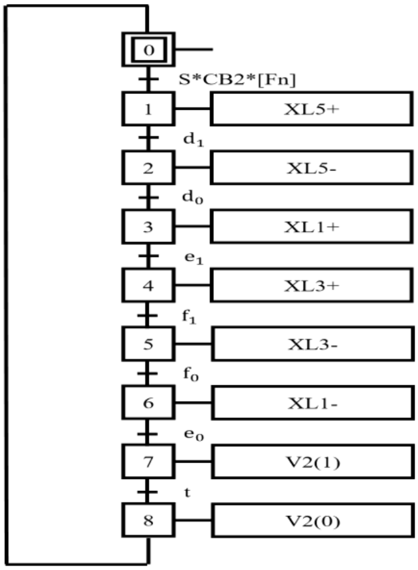

Figure 11. G*RAFCET sequential function chart of the bottle-neck deflashing assembly.*

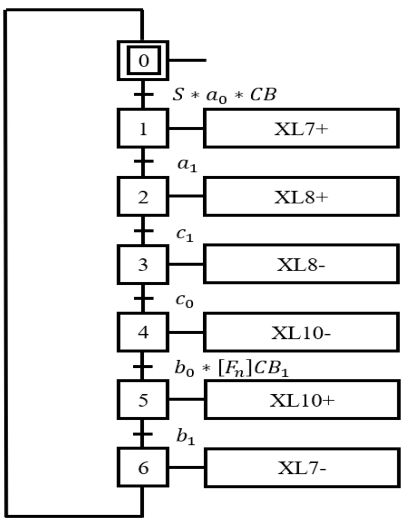

Figure 12. G*RAFCET sequential function chart of the bottle-bottom deflashing assembly*

Figure 13. *Interface of the machine control screen*

5. Results and discussion

The experimental process was conducted on HDPE plastic bottles produced by the extrusion blow molding (EBM) method, with the representative dimensions presented in Table 3. Specifically, the bottles had a height of 70 mm, a diameter of 60 mm, and a wall thickness of 0.4 mm, representing a typical thin-walled bottle configuration commonly used in packaging production. These geometric characteristics impose stringent requirements on the deflashing process to avoid part deformation during processing.

Table 3. *Dimensions of experimental bottles*

Specifications	Value
Bottle height	70 mm
Bottle diameter	60 mm
Bottle wall thickness	0.4 mm

To evaluate the effectiveness of the system, the machine was operated continuously with 100 bottles, after which the products were visually inspected and classified into conforming and non-conforming products.

The defective bottle rate was determined according to the following equation:

$$R = \frac{N_f}{N_t}.100\% = 5\% \quad (10)$$

where Nf is the number of defective bottles and Nt is the total number of tested bottles. The statistical results summarized in Table 4 show that the average processing time for each bottle was approximately 4.5 s, corresponding to a throughput of approximately 800 bottles per hour, with a defect rate of 5%. Experimental observations showed that the trimmed surface at the bottle neck exhibited good quality, with no residual plastic remaining after cutting and no undercut or deformation observed. Similarly, at the bottle bottom, the flash was completely removed without causing deformation of the bottle body or tearing of the material.

Figure 14. *HDPE plastic bottle after deflashing*

Table 4. *Experimental results*

Criteria	Value
Number of bottles	100 bottles
Defect rate	5 %
Cycle time per bottle	4.5 s
Throughput	800 bottles/hour

However, the experiments in this study were mainly intended to verify the feasibility of the prototype model; therefore, the sample size remained limited and was not large enough to fully evaluate the stability and reliability of the system under industrial production conditions. Although the automated deflashing machine for HDPE plastic bottles was successfully designed, fabricated, and tested at the prototype level, the study still has several limitations. Specifically, although the machine is capable of achieving higher throughput, the current stable operating range is approximately 700 bottles per hour. When the processing speed exceeds this level, the defect rate tends to increase, mainly because the bottles have low mass and limited stability, making them prone to positional misalignment during feeding, which leads to bottle jamming in the conveying system.

6. Conclusion

This study proposed and developed the design of an automated deflashing machine for HDPE plastic bottles manufactured by extrusion blow molding technology. Unlike many existing devices that process flash at only a single location, the proposed system enables integrated deflashing at both the bottle neck and bottom within the same device, while maintaining a simple mechanical structure that is easy to manufacture.

The experimental results showed that the machine demonstrated stable operation with a throughput of approximately 700 bottles per hour, demonstrating the feasibility of the design for practical production lines. This design has the potential to be extended to process various types of HDPE plastic bottles with different sizes by adjusting the mechanism parameters.

Compared with existing deflashing machines, the proposed machine enhances the level of automation in production and reduce labor costs and per-unit production cost.

Acknowledgment: This research was funded by the Murata Science Foundation and The University of Danang – University of Science and Technology, under project code T2024-02-01MSF.

REFERENCES

[1] E. Ramakers-van Dorp, C. Blume, T. Haedecke, V. Pata, D. Reith, O. Bruch, B. Möginger, and B. Hausnerova, "Process-dependent structural and deformation properties of extrusion blow molding," *Polymer Testing*, vol. 77, p. 105903, 2019, doi: 10.1016/j.polymertesting.2019.105903.

[2] H. Marshall and W. Reynolds, "*Apparatus for trimming the dome area of a wide mouth blow molded plastic container*," U.S. Patent Application US20040011169A1, Jan. 1, 2004.

[3] T. D. Redies, D. A. Kohler, and L. H. Weber, "*Flash removal apparatus*," U.S. Patent US6358037B1, Mar. 19, 2002.

[4] R. J. Palazzolo, "*Trimmer for removing scraping from tops of plastic bottles,*" U.S. Patent US5257560A, Oct. 19, 1993.

[5] A. J. Thatcher, "*Spin trimmer for removing flashing from the tops of plastic bottle*s," U.S. Patent US4445406A, Apr. 24, 1984.

[6] A. D. Maddox and F. A. Loesch, "*Rotary deflashing apparatus*," U.S. Patent US6360414B1, Mar. 26, 2002.

[7] R. Williams and D. Lockwood, "*Spin trimmer and method of trimmin*g," U.S. Patent Application US20070089573A1, Apr. 26, 2007.

[8] A. J. Thatcher, "*Spin trimming machine with object positioning*," U.S. Patent US4876930A, Oct. 31, 1989.

[9] M. Black, "*Container molding and trimming method and apparatus*," U.S. Patent US4361531A, Jan. 11, 1983.

[10] R. J. Palsa, "*Bottle trimming apparatus*," U.S. Patent US3570087A, Mar. 9, 1971.

[11] J. E. Griesing and D. Weissmann, "*Trimming blow molded plastics articles*," U.S. Patent US3967516A, July 6, 1976.

[12] G. R. Pennington, "*Continuous motion de-flash trimming machine*," U.S. Patent US8881629B2, Nov. 11, 2014.

[13] M. D. Seitz and J. E. Gerdeman, "*Method of and apparatus for handling tandem containers*," U.S. Patent US6675680B1, Jan. 27, 2004.

[14] J. V. Caupena and J. M. Guirado, "*Horizontal cutter of double-bodied bottles attached to each other at the neck*," U.S. Patent US7124673B2, Oct. 24, 2006.

[15] Q. B. Tao, "Design and manufacture a miniature 3-axis CNC wood engraving machine", *UD-JST,* vol. 20, no. 2, pp. 97–101, Feb. 2022.

[16] V. T. Hoang, "Study on the effects of parameters to PET bottle thickness in blowing process", *UD-JST,* vol. 21, no. 12.1, pp. 74–78, Dec. 2023.

[17] J. L. Throne, *Technology of Blow Molding*, 2nd ed., Hanser, 2004.

[18] C. Rauwendaal, *Polymer Extrusion*, 5th ed., Hanser, 2014.

[19] M. A. Osswald and G. Menges, *Materials Science of Polymers for Engineers,* Hanser, 2012.